1.Classification *INPE.COM.10-PE* *CDU: 550.3A*	2.Period *July 1978*	4.Distribution Criterion internal ☐ external ☒ *x*
3.Key Words (selected by the author) *Sodium, Mesosphere.*		
5.Report No. *INPE-1302-PE/146*	6.Date *July, 1978*	7.Revised by *Ivan Jelinek Kantor*
8. Title and Sub-title *THE MESOSPHERIC SODIUM LAYER AT 23°S: NOCTURNAL AND SEASONAL VARIATIONS*		9.Authorized by *Nelson de Jesus Parada* *Director*
10.Sector *DCE/GOA* Code *30.372*		11.No. of Copies 22
12.Authorship *D.M. Simonich* *B.R. Clemesha* *V.W.J.H. Kirchhoff* 13.Signature of first author *Dale Simonich*		14.No. of Pages 44 15.Price

16.Summary/Notes

The vertical profile of mesospheric sodium has been measured by laser radar at São José dos Campos (23°S, 46°W) on 344 nights since 1972. Large day to day variations are observed but averaging over a large number of measurements consistently shows an annual variation by a factor of two in the sodium abundance, with maximum in local winter. The average nocturnal variation is consistent with photochemical control of the bottomside of the layer and diffusive control of the topside. Variations observed on individual nights appear to be mainly dynamic in origin. Vertical structure with a characteristic wavelength of the order of 10 km is frequently seen to propagate downwards through the layer at rates between 1 and 4 km hr^{-1}. Comparison of our results with twilight and daytime absorption abundances suggest a latitudinal assymmetry in the seasonal variation of abundance.

17.Remarks *This work was partially suported by "Fundo Nacional de Desenvolvimento Cientifico e Tecnológico (FNDCT)", Brazil, under contract FINEP-CT/271.*

THE MESOSPHERIC SODIUM LAYER AT 23^{o}S: NOCTURNAL AND SEASONAL VARIATIONS

by

D.M. Simonich, B.R. Clemesha and V.W.J.H. Kirchhoff

Instituto de Pesquisas Espaciais - INPE

Conselho Nacional de Desenvolvimento Científico e Tecnológico - CNPq

12200 - São José dos Campos, SP, Brasil

ABSTRACT

The vertical profile of mesospheric sodium has been measured by laser radar at São José dos Campos (23^{o}S, 46^{o}W) on 344 nights since 1972. Very large day to day variations are observed, both in the total abundance of sodium and in its vertical distribution but, by averaging over a large number of measurements, consistent nocturnal and seasonal trends are observed. An annual variation by a factor of two is observed in the sodium abundance, with maximum in local winter, but no consistent annual variation is seen in the height or shape of the layer, nor in its nocturnal variation. The average nocturnal variation shows a small decrease in abundance before midnight followed by a post-midnight increase. The height of maximum sodium concentration decreases by 2 km during the night, and the scale height of the topside of the layer increases from 2.4 km to 4.7 km. Although the peak concentration of the layer increases slightly during the night, the density at heights below 88 km decreases. These results are consistent with photochemical control of the bottomside of the layer and diffusive control of the topside. Comparison of our results with twilight and daytime absorption abundances, measured at low

northern latitudes, shows a latitudinal assymmetry in the seasonal variation of abundance, suggesting an annual variation in the input of sodium to the upper atmosphere, with a maximum in northern summer. Variations observed on individual nights appear to be mainly dynamic in origin. Vertical structure with a characteristic wavelength of the order of 10 km is frequently seen to propagate downwards through the layer at rates between 1 and 4 km hr^{-1}. This structure appears to be the result of gravity wave and/or tidal perturbations.

1. INTRODUCTION

1.1 - Lidar Characteristics

The mesospheric sodium layer has been observed at São José dos Campos, Brazil ($23^{o}S$, $46^{o}W$) since March 1972. Some preliminary results of these measurements were presented by Kirchhoff and Clemesha (1973). In this paper we present a considerably more complete study, based on 344 nights of measurements made up to August 12, 1977.

The observations have been made using a laser radar tuned to the D_2 line of sodium. The main characteristics of the laser radar are given in Table 1.

TABLE 1

SPECIFICATIONS OF THE LASER RADAR

Transmitted energy	20 mJ
Pulse duration	2 μs
Maximum Repetition rate	0.5 s^{-1}
Wavelength	589.0 nm
Total transmitted bandwidth	12 pm
Receiver area	0.39 m^2
Receiver bandwidth	1 nm
Receiver efficiency	2 %
Normal height interval	2 km

The laser is kept tuned to the D_2 line by an automatic tuning system (Clemesha et al., 1975). This system uses a piezoelectric Fabry-Perot interferometer in a servo loop to tune the laser to a sodium lamp reference.

1.2 - Lidar Calibration

Following Kent et al. (1967) we may express the signal produced in the receiver of a lidar by scattering from atmospheric molecules as

$$C(h) = \frac{n(h)\ \rho\ K\ T^2}{h^2} \qquad (1)$$

where

$C(h)$ = the number of photons detected from height h per km per shot;

$n(h)$ = the number density of scattering molecules at height h;

ρ = the Rayleigh backscatter function per molecule;

T = the total atmospheric transmission from the lidar to height h;

K = a constant of the lidar.

Our lidar simultaneously measures the resonant scattering from the sodium layer and the Rayleigh scattering from the stratosphere. Since almost all of the atmospheric attenuation takes place in the troposphere, taking the ratio of these two signals causes the factor KT^2 to cancel out giving

$$\frac{C(h_1)}{C(h_2)} = \frac{Na(h_1)\ \rho_{Na}\ h_2^2}{D(h\ )\ \rho_R\ h_1^2} \tag{2}$$

$$Na(h_1) = \frac{C(h_1)\ D(h_2)\ \rho_R\ h_1^2}{C(h_1)\ \rho_{Na}\ h_2^2} \tag{3}$$

where

$Na(h_1)$ = the number density of sodium atoms at height h_1;

$D(h_2)$ = the atmospheric molecular number density at height h_2;

ρ_{Na} = the effective resonant backscatter function for sodium atoms;

ρ_R = the average Rayleigh backscatter function for atmospheric molecules in the stratosphere.

We have used an average value for $D(h_2)$ obtained from local radiosonde measurements. Seasonal and day to day variations in the density at 25 km, the value usually chosen for h_2, are only a few percent at our latitude, and have been neglected. A more serious error might be introduced by aerosol scattering. This has been taken into account by fitting our measured stratospheric scattering profile, typically extending from 14 km to 44 km, to a standard atmosphere in order to determine the aerosol scattering ratio at the height h_2. Details of this procedure have been given by Clemesha and Simonich (1978).

In order to determine the effective resonant backscatter function for the sodium atoms, equal to $\sigma_{eff}/4\pi$, where σ_{eff} is the effective resonant scattering cross-section, we must accurately determine the transmitted spectrum. The bandwidth for the early data was obtained by measurements of the laser spectrum using spectrographic techniques. After December 1974 a sodium vapor cell and a total energy monitor were added to the system. These measure both the total energy of the laser and the energy available for resonant scattering. The scattering cell is used to measure the laser bandwidth as well as to monitor short term changes in the laser spectrum during actual data taking.

The laser bandwidth is obtained by sweeping the laser through the D_2 line in known wavelength increments using the piezoelectric Fabry-Perot interferometer. If the laser spectrum is assumed to be gaussian and the absorption cross-section for the sodium D_2 line is represented by a double gaussian (Chamberlain, 1961), the analytic expression resulting from the convolution $S(\tau)$ of the laser spectrum with the absorption

cross-section is

$$S(\tau) = \frac{W_o \beta}{\sqrt{\alpha^2+\beta^2}} \{N_a \exp[-(\tau - \lambda_a)^2/(\alpha^2+\beta^2)] +$$

$$+ N_b \exp[-(\tau + \lambda_b)^2/(\alpha^2+\beta^2)]\} \qquad (3)$$

where

τ = wavelength displacement from 589 nm in pm;

W_o = the transmitted energy;

α = the 1/e half-width of the laser spectrum in pm;

β = the 1/e half-width of the Doppler broadened D_2 line

$(5.28 \times 10^{-2} \sqrt{T}$ pm);

$N_a = 1.33 \times 10^{-14} / \sqrt{T}$ m^2;

$\lambda_a = 0.73$ pm;

$N_b = 7.965 \times 10^{-15} / \sqrt{T}$ m^2;

$\lambda_b = 1.23$ pm;

T = the temperature of the sodium atoms in ^oK.

The experimental data can be fitted to this equation to get the laser bandwidth. The effective scattering cross-section is given by

$$\sigma_{eff} = \int N(\lambda)\, L(\lambda)\, d\lambda \;/\; \int L(\lambda)\, d\lambda$$

where

$N(\lambda)$ = the resonant scattering cross-section of the sodium atoms;

$L(\lambda)$ = the laser spectrum.

Using the previous assumptions, this can be calculated as

$$\sigma_{eff} = \frac{\beta}{\sqrt{\alpha^2+\beta^2}} \{N_a \exp[-\lambda_a^2/(\alpha^2+\beta^2)] +$$

$$+ N_b \exp[-\lambda_b^2/(\alpha^2+\beta^2)]\} \qquad (5)$$

where β, N_a and N_b are evaluated at the mesospheric temperature (200^o K).

The scattering cell system is also used during measurements to monitor short term changes in the laser. If the ratio of the energy scattered by the sodium vapor to the total laser energy increases as compared to the ratio obtained during the bandwidth measurement, the bandwidth of the laser must have decreased. If the ratio decreases, it is due either to an increase in the bandwidth of the laser or to the laser being slightly off the center of the D_2 line. These effects are taken into account by a correction to the effective scattering cross-section:

$$\sigma_{eff} = \frac{Na/W}{Na^o/W^o} \sigma^o_{eff} \qquad (6)$$

where

σ_{eff} = the corrected effective cross-section;

Na = the average scattered signal from vapor cell during sodium measurement;

W = the average laser energy during sodium measurement;

Na^o = the scattered signal from the vapor cell during bandwidth measurement;

W^o = the laser energy during bandwidth measurement;

σ^{o}_{eff} = the effective cross-section obtained during bandwidth measurement.

Equation 6 would be exact only if the temperature of the sodium atoms in the scattering cell were equal to that in the mesosphere. In practice our scattering cell operates at 420°K, as against a typical mesospheric temperature of 200°K. We calculate, however, that the error introduced by this difference does not exceed 1%, mainly because the bandwidth of our laser is much larger than that of the measured line.

The main source of error in our calibration procedure lies in the determination of the laser bandwidth, which we believe to be accurate to approximately ± 10%. Other sources of error, such as the uncertainty in the stratospheric scattering, are much smaller and can be neglected. Before the installation of the scattering cell, errors in the bandwidth determination may have been as large as ± 40% for individual measurements, although for averages over many days it is unlikely that the error would have been more than ± 20%.

2. RESULTS

2.1 - General Characteristics of the Layer

Figure 1 shows a series of profiles of the sodium layer averaged over different time intervals. Individual profiles are generally obtained by accumulating the returns from 50 shots of the laser during a time interval of approximately 3 minutes. The error

bars shown in the figure are proportional to the square root of the photon count at each height and thus correspond to the probable statistical error in the measurement. The data have been corrected for resonant absorption in the layer. The altitudes shown in the figures are height above sea level.

Figure 1a shows a single 50 shot profile from the night of July 31, 1975, taken at 2218 LST. The profile shows a considerable amount of structure with 2 distinct peaks. Profiles with this integration time ($\sim$ 3 min) generally show complex structure.

Figure 1b shows an average of 6 profiles taken on the same night between 2200 and 2300 LST. The small scale structure has disappeared but the two peaks remain. This double peaked structure is quite common in our data averaged over short time periods. On occasions as many as three peaks may be maintained for several hours, but never over an entire night. In this respect our results are quite similar to those of Sandford and Gibson (1970) in England, and Blamont et al. (1972) in France.

Figure 1c shows the average of all the profiles obtained on the night of July 31, 1975, over a period of seven hours. The distinct double peaked structure continues to be visible, although the minimum between the peaks has been filled in. The maintenance of a minimum between two peaks when the data is averaged over many hours is not common, although the plateau type structure shown occurs frequently.

Figure 1d shows the average of the nights of July 30 and 31, 1975. Observations were made during only 4 hours on July 30 but the general shape of the layer was similar to that seen on July 31. Normally there is a certain amount of continuity of the profile from night to night, although radical changes in the layer are not uncommon. Sometimes the layer structure remains similar for three or four consecutive nights.

Figure 1e is the average for all the days on which observations were made in July of 1975. This curve shows a very smooth variation with height with the plateau type structure still in evidence. Finally, in Figure 1f, we show the average profile for 1975. It is interesting to note that although the average layer shows a sharp maximum at 94 km, a tendency towards a secondary maximum at 85 km is still visible.

2.2 - Seasonal Variation

The bottom part of Figure 2 shows the mean monthly profiles in the form of a contour plot where the averaging was carried out over all five years of data. In determining the monthly means, equal weight was given to each night's data regardless of the duration of measurement. Note that the January data is repeated in order to show the complete annual cycle. Because of frequent cloud cover during summer, the number of nights of data included in each monthly average varies from a minimum of 11 in December to a maximum of 56 in July with an average value of 28.7 days. The dashed curve is the height of the maximum density for each monthly average. The upper part

of Figure 2 is the monthly mean abundance curve.

There appears to be no significant seasonal variation in the height or structure of the layer. Minimum densities occur in December at the beginning of summer. Subsequently the density increases proportionally at all heights reaching a broad maximum beginning in April. The densities remain high until October when the layer begins its decrease to the summer minimum. The abundance shows the same general behavior, a relatively sharp minimum at the beginning of summer and a broad maximum almost from equinox to equinox.

Figure 3 shows a mass plot of the average nightly abundance for all available data. The smooth curve drawn through these points is a three point running mean of the monthly average abundance. The summer minimum in abundance is clearly evident for each year in which we have made measurements. Also evident are the large day to day variations of the abundance. The form of the annual variation also changes considerably from year to year.

The dashed curve in Figure 3 is a least mean squares fit of a function containing 1 year and 11 year periods. This curve represents the function

$$A(t) = 4.38 - \cos\left(2\pi \frac{t+6}{365}\right)\left[1.16 + 0.27 \cos\left(2\pi \frac{t+77}{4015}\right)\right] +$$

$$+ 0.61 \cos\left(2\pi \frac{t+77}{4015}\right) \qquad (6)$$

where

$A(t)$ = the abundance in units of 10^{13} m^{-2}

t = the time in days from January 1, 1973

The yearly cycle shows a minimum very close to the beginning of the year. The 11 year cycle has a minimum in early 1978. The minimum of the solar cycle occurred in 1976. Our choice of an eleven year cycle to represent the long term variation visible in Figure 3 is, of course, arbitrary, and more data will be necessary in order to determine whether there really exists a sunspot cycle variation in the sodium layer.

2.3 - Day to Day Variations

Figure 4 shows a contour plot of sodium densities for the period of 15 days from July 20 to August 3, 1976, during which period observations were made on every night except July 21. The contours are plotted through the nightly averages, each of which represents the mean of at least 9 hours of observations. It can be seen from Figure 4, that the distribution shows appreciable continuity over a period of several days, although large changes sometimes occur from one night to the next, as in the case of the 28th - 29th July, where an abundance increase by a factor of 1.35 is accompanied by a major change in the vertical distribution of sodium.

2.4 - Nocturnal Variations

Figure 5 shows a contour plot of the half-hour average

profiles for the night of July 25-26, 1976. Also shown is the abundance curve for these half-hour values. The predominant feature visible in this figure is the decrease in the height of peak density throughout the night. Less obvious is the existence of secondary peaks, approximately 10 km below the main peak, from 1900 to 2200 hours, and 10 km above the main peak between 0200 and 0600 hours, descending at the same rate as the main peak. The descending structure appears to represent a wave motion with a vertical wavelength of the order of 10 to 12 km, whose phase descends at the rate of 1 km hr^{-1}. Although the night of July 25-26, 1976, was chosen as a particularly clear example of a descending wave motion, most of our measurements show a structure which descends with time at a rate between 1 and 4 km hr^{-1}, and with a vertical wavelength of the order of 10 km. The phase of this wave varies greatly from night to night, however, and its existence is not apparent in the average nightly behaviour shown in Figure 6.

The derivation of an average nocturnal variation is complicated by the fact that most of our observations refer to time periods of only a few hours for any given night. As a result of this, the very large night to night variations which frequently occur will tend to introduce spurious nocturnal variations if a simple average is taken. In order to overcome this problem we have averaged the fractional rate of change of total abundance measured at hourly intervals, and have integrated these average values to give a mean nocturnal variation of total abundance. Individual profiles were subsequently normalized to this mean abundance variation and then averaged to obtain the mean nocturnal variation of the sodium distribution.

The average abundance curve shown in the upper part of Figure 6, shows only a very small nocturnal variation of about 4% with a minimum abundance of $4.8 \times 10^{13} m^{-2}$ just before midnight. The vertical distribution of sodium undergoes significant changes during the night. At heights above 100 km there is a considerable increase in density, mainly after midnight. Between 1900 and 0500 LST the density increases by a factor of 4 at 104 km and by a factor of 19 at 106 km. At heights below 90 km there is a steady decrease in density throughout the night. At 84 km, for example, the density at 0500 LST is only 50 % of that at 1900 LST. The peak density changes by about 12 % during the night, with a maximum occurring at 0300 LST. The height at which the maximum density occurs decreases monotonically from about 95 km at 1900 LST to 93 km at 0500 LST.

2.5 - Correlation with Geophysical Parameters

The mean nightly abundance was compared with ΣK_p (centered on local midnight), solar flux and sunspot number with time shifts of up to ± 30 days. No significant correlation was found between abundance and geomagnetic activity. A small correlation with the other two parameters was found. The correlation coefficient between abundance and solar flux varies between 0.106 and 0.189 with a mean value of 0.15. With sunspot number the correlation coefficient varies between 0.116 and 0.26 with a mean of 0.18. Both of these correlations are significant at the 1 % level. These correlations are undoubtably the result of the long term trend in sodium abundance and the solar cycle variations in solar flux and sunspot number. As our data are insufficient

to determine whether or not the trend is part of a solar cycle variation, we cannot know whether or not the correlations are physically significant.

3 - DISCUSSION

3.1 - Vertical Structure

Individual profiles, which normally represent a time average of 3 to 5 min, show a considerable amount of fine structure which disappears when longer averaging times are considered. These fluctuations could either be caused by a wave disturbance, or by the horizontal movement of spatial irregularities in the layer. The existence of horizontal structure in the mesosphere has been shown by observations of the OH nightglow (Krassovsky, 1977). Attempts to investigate the horizontal structure in the sodium layer have been made by Thomas et al., (1976), who used a steerable laser radar to measure the vertical distribution of sodium at locations separated by distances from 15 to 100 km. Their results showed little small scale spatial or temporal variation over periods up to 1 hour, other than a vertical oscillation of the entire layer. We have also made spaced observations at 3 positions with the intention of measuring horizontal motions by the technique first developed for ionospheric drift measurements by Mitra (1949). These measurements were made in early 1974, before the installation of the scattering cell calibration system, and thus their analysis is hampered by the apparent fluctuations in sodium abundance produced by the uncompensated short term fluctuations in the spectral output of the laser. They do show, however, that the detailed structure

3.2 - Seasonal Behavior

Our observation of a winter maximum in abundance is in agreement with the twilight observations as summarized by Hunten (1967) and the lidar measurements of Gibson and Sandford (1971) and Megie and Blamont (1977). The details of the seasonal variation are, however, rather different. Both Gibson and Sandford, working at Winkfield, England (51^{o}N), and Megie and Blamont, at Haute-Provence, France (44^{o}N), find that the winter maximum is confined to a few months of the year only, with little change outside of these months. Our observations indicate a broad maximum from early autumn to late spring. The winter maximum in density observed at northern midlatitudes appears to result from a large increase in sodium density on the bottomside of the layer. This is particularly evident in the case of the Winkfield results, and is implied by a winter lowering of the layer observed at Haute-Provence. We observe no significant seasonal variation in the vertical distribution of sodium at our latitude. Although the Winkfield results are for only one year, the Haute-Provence observations cover a period of nearly 3 years, and it seems probable that the differences noted above are genuine latitudinal effects.

The sodium abundance varies by about a factor of 2 from summer to winter at our latitude. This ratio appears to be about 3:1 at Haute-Provence, and 4:1 at Winkfield. Twilight observations made at Tamanrassett (23^{o}N) show no significant seasonal variation, which is surprising, since one would expect to see a seasonal effect similar to that at 23^{o}S, with a 6 month phase lag.

There appears to be a northern to southern hemisphere assymmetry in the magnitude of the seasonal variation in sodium abundance. In Figure 7, we present the ratio of the average December-January abundance to the average June-July abundance for a number of stations. Table II gives the observational data for each station. The dots are data from twilight resonant scattering measurements. The data have been reduced (or rereduced where necessary) to sodium abundance using Figure 5 of Hunten (1967), with a day to twilight abundance ratio of 1. Hunten et al. (1964) report that their data for Christchurch has some uncertainty in the calibration as well as other problems. Therefore the sparse data of Tinsley and Vallance Jones (1962) are included (circle). Note that this point is much closer to the ratio at Lauder, at almost the same latitude, and therefore we tend to discount the Hunten et al. data point. The squares are daytime solar absorption measurements. Because of the large error bars compared to the variation of the data points, the Boca Raton ratio was obtained by averaging the bimonthly values covering the appropriate two month periods. The crosses are the laser radar data.

It can be seen from Figure 7 that there is an appreciable difference in the winter/summer ratios between low latitude stations in the northern and southern hemispheres. This difference could either result from the different measuring techniques used, or could point to an annual variation in sodium input. The low latitude northern hemisphere results are from daytime absorption or twilight measurements. If there exists an appreciable difference between the seasonal variations of the daytime and nighttime abundances then this would appear in Figure 7 as an apparent

latitudinal effect. The dayglow measurements (Blamont and Donahue, 1961) originally suggested a considerable enhancement of sodium abundance during the day, but it now appears that the interpretation of these measurements was in error (Chanin and Goutail, 1975). Both the absorption and dayglow measurements reported by Burnett et al. (1972) and Burnett et al. (1975), show no diurnal variation. On the other hand Partowmah and Roesler (1977) consider that their absorption measurements show a diurnal variation which is strongest in winter. The sense of Partowmah and Roesler's diurnal variation is such, however, as to suggest that the seasonal variation of the nighttime abundance is less than that of the daytime abundance. This would indicate a seasonal variation smaller than that observed by other techniques at latitudes around $44^{o}N$, and thus would increase, rather than decrease the latitudinal assymmetry. Gibson and Sandford (1972) have made a limited number of daytime lidar measurements and also find no consistent difference between daytime and nighttime abundance. It is also significant that the seasonal variation in the twilight abundance of Haute Provence is very similar to the seasonal variation in the nighttime abundance measured by lidar.

Although the evidence is not conclusive it does appear to point to a latitudinal assymmetry in the seasonal variation of sodium abundance. If such an assymmetry exists it suggests an annual variation in the input of sodium, with a maximum input in northern summer, so that the annual and seasonal variations would tend to cancel at low northern latitudes and reinforce each other at low southern latitudes. One of the possible sources for the sodium layer is meteoric influx. Radio meteor studies do, in fact, show an annual variation in meteor

rates (Hawkins, 1956; Elford, 1967). Unfortunately the variation does not appear to be in the right phase, since it shows a maximum influx between July and December, rather than in northern summer. Possibly incoming particles which contribute most to the sodium layer have an annual variation different from that of radio meteors.

The seasonal variation of mesospheric sodium might be explained, at least in part, by the seasonal temperature variations in this region. From the US Standard Atmosphere Supplements, 1966, we estimate that the yearly temperature variation at an altitude of 90 km is 11°K (174 - 185°K) at 23° latitude, while it is 38°K (163-201°K) at 51° latitude. The main photochemical reactions of sodium are thought to be (Hunten, 1967)

$$Na + O_3 \rightarrow NaO + O_2;\ k_1 = 5.16 \times 10^{-10} \exp\left[-\frac{875}{T}\right]\ cm^3 s^{-1} \qquad (7)$$

$$NaO + O \rightarrow Na^* + O_2;\ k_2 = 3 \times 10^{-7} \exp\left[-\frac{1790}{T}\right]\ cm^3 s^{-1} \qquad (8)$$

where the values for the temperature dependent rate coefficients are from Megie (1976). In equilibrium

$$\frac{[Na]}{[NaO]} = \frac{k_2[O]}{k_1[O_3]} \qquad (9)$$

where the brackets indicate densities. Model calculations by Shimazaki and Laird (1972) suggest that there is no seasonal variation in the $[O]/[O_3]$ ratio. The ratio k_2/k_1, and therefore the ratio $[Na]/[NaO]$ changes by a factor of 1.3 from summer to winter at 23° latitude, while at 51°

latitude it changes by a factor of 2.9 for the temperature variations given above. The main difficulty with this argument is the fact that if the absolute values of k_1 and k_2 normally accepted are correct, only a small fraction of the sodium would be in the form of the oxide, so that changes in the [Na]/[NaO] ratio would have little effect on the abundance. It should be pointed out, however, that Kolb and Elgin (1976) have suggested that the reactions between sodium and oxygen proceed by the electron jump mechanism, and this would imply a value for k_1 about 50 times larger than that normally used. Since k_2 would be increased by only a factor of 4, the ratio of NaO to O would be increased by more than a factor of 10, with the result that photochemical changes could have a greater effect on the sodium density. It appears to us to be particularly significant that the large winter increase in sodium abundance, observed at mid-latitudes, results mainly from an increase in density on the bottomside of the layer, where photochemistry is most likely to be important.

3.3 - Nocturnal Variation

The average nocturnal variation shown in Figure 6 appears to be the result of various processes occurring in different height regions. Perhaps the most notable feature of the average nocturnal variation is the increase in the topside scale height during the night. The scale height measured at a height of 100 km, increases from 2.4 km at 1812 LST to 4.7 km at 0506 LST. Since the scale height of the Na layer is much smaller than that of the main constituents of the atmosphere, it is possible to explain its increase as being caused by

diffusion. The fact that the topside scale height of the sodium layer is much less than the atmospheric scale height has received considerable attention in the literature. Attempts to explain the smallness of the scale height on the basis of a thin source layer have been made by Hunten and Wallace (1967) and Donahue (1966). The source layer is supposed to consist of aerosols from which sodium evaporates, mainly during the day. An alternative explanation on the basis of the ionization of sodium has been suggested by Hanson and Donaldson (1967). An increase in scale height during the night, when the aerosol source or ionization sink mechanism would be turned off, is consistent with either of these two mechanisms, and thus our observations do not help to distinguish between them.

The decrease of approximately 2 km in the height of peak sodium density during the night, visible in Figure 6, can also be explained on the basis of diffusion. The height of maximum mixing ratio, 97 km, does not, in fact, change by more than 0.5 km from 1900 LST to 0500 LST.

As in the case of the seasonal variation, the loss of sodium on the bottomside of the layer during the night could be due to a decrease in the [Na]/[NaO]ratio. Model calculations (Shimazaki and Laird, 1972) suggest that a large nocturnal decrease in the atomic oxygen density occurs at heights below 88 km, and thus the lack of sodium oxide, which photochemical equilibrium using the normally accepted rate coefficients suggests, is not quite so serious an objection as in the case of the seasonal variation. Nevertheless, model calculations

by Megie (1976) show negligible nocturnal variation in sodium density on the bottomside of the layer. The cessation of both O_2 dissociation and O_3 photolysis should result in a large decrease in the $[O] / [O_3]$ ratio at sunset, but photochemical model calculations do not suggest that this ratio should continue to decrease during the night. It seems, then, that although the day to night change in the $[O] / [O_3]$ ratio is in the right sense to explain a decrease in sodium density at sunset, it is difficult to see why this decrease should continue throughout the night.

Although the density on the bottomside of the sodium layer generally decreases during the night, the peak density reaches a maximum at about 0300 LST. The total variation of the peak density is quite small, being about 7% in the case of the all-season average shown in Figure 6. Takahashi et al. (1977) have reported average nocturnal variations in the OH (8,3) band and OI 5577Å nightglow emissions showing maximum intensities just after 0300 LST. These workers point out that the $\Theta_2^{2\omega,2}$ fundamental mode of the solar semi-diurnal tide should result in maximum atmospheric density at 0300 LST, and suggest that the tide may be responsible for a major part of the nocturnal variation in the emission intensities. The $\Theta_2^{2\omega,2}$ mode at our latitude should have an amplitude of about 8% at 94 km, and thus is of the right order of magnitude to explain the sodium peak density variation as well.

The total abundance of sodium varies by about 2.5% reaching a minimum just before midnight. Although this variation is

small, it should be pointed out that it is the result of a comparatively large decrease on the bottom of the layer and an increase at the top. The sodium content below 90 km decreases during the night from 7.0 to 5.4×10^{13} m^{-2} (23%), whereas the content above this height increases from 17.8 to $19.4 \times 10^{13} m^{-2}$ (9%). The post-midnight increase in abundance means that the loss of sodium below 88 km must be more than compensated by an increase at greater heights. This increase could either be due to recombination of Na^+ ions, or could result from increased meteoric input. It appears to be difficult to distinguish between these two possibilities because both would lead to increased sodium density on the topside of the layer. The meteoric influx mechanism is, perhaps, favored by the fact that the sporadic meteor flux should have its maximum strength at 0600 LST.

The features of the nocturnal behavior of the sodium layer discussed above are consistently distinguishable only in the average of many nights data. On individual nights the behaviour of the layer appears to be dominated by dynamical effects. It has been suggested that the descending wave structure may be due to gravity waves (Blamont et al., 1972) or tides (Kirchhoff and Clemesha, 1973). The principal diurnal tidal modes which we expect to observe in the mesosphere at our latitude are the $\Theta_1^{\omega,1}$ and $\Theta_3^{\omega,1}$ modes, with vertical wavelengths of 25 km and 12 km respectively. A detailed analysis of the dynamical behavior of the sodium layer will be presented elsewhere, but it is worth mentioning here that the main characteristic wavelengths which we observe are about 20 km and 11 km. The phase of the oscillation varies greatly from night to night and it is not

observed in the average variation presented in Figure 6. Large phase and amplitude variations in the diurnal tide are observed in low latitude meteor wind measurements (Scholefield and Alleyne, 1975).

4. CONCLUSIONS

The average sodium layer measured at 23^{o}S shows a peak sodium density of 3.6×10^{9} m^{-3} at about 94 km, and a width of 13.7 km between 1/e points. The average total abundance of sodium in a vertical column is 4.4×10^{13} m^{-2}. There is a tendency for a subsidiary peak to occur at a height of about 85 km. If this subsidiary peak is related to a minimum in the mesospheric ozone distribution, then it is inconsistent with presently accepted ozone models.

The nocturnal variation in the sodium layer on individual nights, shows the existence of vertical structure which propagates downwards at rates between 1 and 4 km hr^{-1}. This structure shows characteristic lengths of about 11 and 20 km.

The average nocturnal variation shows an increase in the topside scale height (measured at 100 km) from 2.4 km at 1812 LST to 4.7 km at 0506 LST. Both this increase in the scale height and a decrease of 2 km in the height of the peak sodium density are consistent with diffusive control of the upper part of the layer during the night. At heights below 88 km the sodium density decreases during the night. In the region of 80 to 82 km the density at 0500 LST is less than one half of the density at 1900 LST.

The seasonal variation in total abundance shows a winter maximum when the abundance is about twice its value at the summer minimum. The variation for individual years is irregular, but the average for 5 years shows a fairly sinusoidal seasonal behavior, and does not present the sharp winter increase seen at midlatitudes in the northern hemisphere. We see no consistent seasonal variation in the height or the shape of the layer. Although there is some day to day continuity, both in the layer shape and abundance, changes in the abundance by a factor of more than two can occur over a period of a few days.

Comparing our results with the twilight and daytime absorption abundances measured at low northern latitudes, we find a latitudinal assymmetry in the seasonal behavior. Assuming that there are no large differences between the daytime or twilight abundances and the nighttime abundances, there appears to be an annual variation in sodium input, with a maximum occurring during northern summer.

ACKNOWLEDGEMENTS

We would like to thank Mr. Paulo Prado Batista for helping with some of the observations. This work was partially supported by the Fundo Nacional de Desenvolvimento Científico e Tecnológico (FNDCT) under contract FINEP CT/271.

TABLE II

OBSERVATIONAL DATA FOR FIGURE 7

LATITUDE	STATION	TYPE	TIME-PERIOD	REFERENCES
59°N	CHURCHILL	TWILIGHT	1956-1959	HUNTEN (1967)
51°N	SASKATOON	TWILIGHT	OCTOBER 58-JUNE 63	HUNTEN (1967)
51°N	WINKFIELD	LIDAR	JULY 69-JULY 70	GIBSON AND SANDFORD (1971)
48°N	VICTORIA	TWILIGHT	FEB. 67-JULY 68	SULLIVAN (1971)
44°N	HAUTE-PROVENCE	TWILIGHT	1954-1963	BLAMONT AND DONAHUE (1964)
44°N	HAUTE-PROVENCE	LIDAR	OCT. 73-JULY 76	MEGIE AND BLAMONT (1977)
43°N	MADISON	ABSORPTION	1971-1974	PARTOWMAH AND ROESLER (1977)
32°N	KITT PEAK	TWILIGHT	APRIL 64-APRIL 66	HUNTEN (1967)
26°N	BOCA RATON	ABSORPTION	1967-1971	BURNETT ET AL. (1972)
23°N	TAMANRASSET	TWILIGHT	1958-1959	DONAHUE AND BLAMONT (1961)
23°S	SÃO JOSÉ DOS CAMPOS	LIDAR	1972-1977	THIS PAPER
44°S	CHRISTCHURCH	TWILIGHT	1961-1962	HUNTEN ET AL. (1964)
44°S	CHRISTCHURCH	TWILIGHT	1960	TINSLEY AND VALLANCE-JONES (1962)
45°S	LAUDER	TWILIGHT	1962-1963	GADSDEN (1964)

REFERENCES

BLAMONT, J.E. and T.M. DONAHUE. The Dayglow of the Sodium D Line. *J. Geophys. Res.*, 66, 1407-1423, 1961.

BLAMONT, J.E. and T.M. DONAHUE. Sodium Dayglow: Observation and Interpretation of a Large Diurnal Variation. *J. Geophys. Res.*, 69 4093-4127, 1964.

BLAMONT, J.E., M.L. CHANIN and G. MEGIE. Vertical Distribution and Temperature Profile of the Night Time Atmospheric Sodium Layer obtained by Laser Backscatter. *Ann. Geophys.*, 28, 833-838, 1972.

BURNETT, C.R., W.E. LAMMER, N.T. NOVAK and V.L. SIDES. Absorption Measurements of Upper Atmospheric Sodium at Boca Raton, Florida, 1967-1971. *J. Geophys. Res.*, 77, 2934-2941, 1972.

BURNETT, C.R., R.W. LASHER, A.A. MISKIN, and V.L. SIDES. Spectroscopic Measurement of Sodium Dayglow: Absence of a Large Diurnal Variation. *J. Geophys. Res.*, 80, 1837-1844, 1975.

CHANIN, M.L. and J.P. GOUTAIL. Diurnal Variation of the Sodium Dayglow. *J. Geophys. Res.*, 80, 2854-2858, 1975.

CHAMBERLAIN, J.W. Physics of the Aurora and Airglow. *International Geophysics Series V.2.* Academic Press, New York, 1961.

CLEMESHA, B.R., V.W.J.H. KIRCHHOFF and D.M. SIMONICH. Automatic Wavelength Control of a Flashlamp-pumped dye Laser. *Optical and Quantum Electronics*, 7. 193-196, 1975.

CLEMESHA, B.R. and D.M. SIMONICH. Stratospheric Dust Measurements, 1970-1977. *J. Geophys. Res.* In press, 1978.

CLEMESHA; B.R., V.W.J.H. KIRCHHOFF and D.M. SIMONICH. Simultaneous Observations of the Na 5893Å Nightglow and the Distribution of Sodium Atoms in the Mesosphere. *J. Geophys. Res.* In Press, 1978.

DONAHUE, T.M. and J.E. BLAMONT. Sodium in the Upper Atmosphere. *Ann. Geophys*, 17, 116-133, 1961.

DONAHUE, T.M. On the Ionosphere conditions in the D Region and Lower E Region. *J. Geophys. Res.*, 71, 2237-2242, 1966.

ELFORD, W.G. Incidence of Meteors on the Earth Derived from Radio Observations, Meteor Orbits and Dust; The Proceedings of a Symposium. Edited by G.S. Hankins, NASA, Washington DC., 1967.

GADSDEN, M. On the Twilight Sodium Emission-1. Observations from a Southern Hemisphere Station. *Ann. Geophys*, 20, 261-272, 1964.

GIBSON, A.J. and M.C.W. SANDFORD. The Seasonal Variation of the Night-time Sodium Layer. *J. Atmos. Terr. Phys.*, 33, 1675-1684, 1971.

GIBSON, A.J., and M.C.W. SANDFORD. Daytime Laser Radar Measurements of the Atmospheric Sodium Layer. *Nature*, 239, 509-511, 1972.

HANSON, H.B., and J.S. DONALDSON. Sodium Distribution in the Upper Atmosphere. *J. Geophys. Res.*, 72, 5513-5514, 1967.

HAWKINS, G.S. A Radio Echo Survey of Sporadic Meteor Radiants. *Notices Roy. Astron. Soc.*, 116, 92-104, 1956.

HUNTEN, D.M., A. VALLANCE-JONES, C.D. ELLYETT, and E.C. MCLAUCHLAN. Sodium Twilight at Christchurch, New Zealand. *J. Atmos. Terr. Phys.*, 26, 67-76, 1964.

HUNTEN, D.M. Spectroscopic Studies of the Twilight Airglow. *Space Sci. Revs.*, 6, 493-573, 1967.

HUNTEN, D.M. and L. WALLACE. Rocket Measurements of the Sodium Dayglow. *J. Geophys. Res.*, 72, 69-79, 1967.

KENT, G.S., B.R. CLEMESHA, and R.W. WRIGHT. High Altitude Atmospheric Scattering of Light from Laser Beam. *J. Atmos. Terr. Phys.*, 29, 169-181, 1967.

KIRCHHOFF, V.W.J.H., and B.R. CLEMESHA. Atmospheric Sodium Measurements at 23^{o}S. *J. Atmos. Terr. Phys.*, 35, 1493-1498, 1973.

KOLB, C.E., and J.B. ELGIN. Gas Phase Chemical Kinetics of Sodium in the upper Atmosphere. *Nature*, 263, 488-489, 1976.

KRASSOVSKY, V.I. Internal Gravity Waves near the Mesopause and the Hydroxyl Emission. *Ann. Geophys.*, 33, 347-356, 1977.

MEGIE, G. Contribution à l'Étude du Comportement de l'Atmosphère à la Mésopause obtenue par Sondage Laser du Sodium, Ph.D. Thesis l'Université Pierre et Marie Curie, Paris, 1976.

MEGIE, G. and J.E. BLAMONT. Laser Sounding of Atmospheric Sodium: Interpretation in terms of Global Atmospheric Parameters. *Planet. Space. Sci.*, 25, 1093-1109, 1977.

MITRA, S.N. A Radio Method of Measuring Winds in the Ionosphere. *Proc. Inst. Elec. Eng.*, 96-III, 441-446, 1949.

PARTOWMAH, M. and F.L. ROESLER. Absorption Studies of Daytime Sodium Abundance. *J. Geophys. Res.*, 82, 2607-2612, 1977.

RIEGLER, G.R., S.K. ATREYA, T.M. DONAHUE, S.C. LIU, B. WASSER and J.F. DRAKE. UV Stellar Occultation Measurements of Nighttime Equatorial Ozone. *Geophys. Res. Letters*, 4, 145-148, 1977.

SANDFORD, M.C., and A.J. GIBSON. Laser Radar Measurements of the Atmospheric Sodium Layer. *J. Atmos. Terr. Phys.*, 32, 1423-1430, 1970.

FIGURE CAPTIONS

Fig. 1 - Sodium profiles for different averaging times: (a) 3 minutes; (b) 1 hour; (c) 7 hours (all from July 31, 1975); (d) July 30 and 31, 1975; (e) month of July, 1975; (f) 1975 average.

Fig. 2 - Average seasonal variation of sodium density and abundance. The density contour interval is 0.5×10^9 m^{-3}. The broken curve is the height of maximum density.

Fig. 3 - Mass plot of mean nightly abundances. The solid curve represents a 3 month running mean and the broken curve is the best fit sinusoid.

Fig. 4 - Average nightly abundance and density variation for the period July 20 to August 3, 1976. The contour interval is 0.5×10^9 m^{-3}.

Fig. 5 - Nocturnal variation of abundance and density, July 25-26, 1976. The contour interval is 0.5×10^9 m^{-3}.

Fig. 6 - Mean nocturnal abundance and density variations derived from all data. The contour interval is 0.5×10^9 m^{-3} except for the broken curves which are as indicated.

Fig. 7 - Variation of the ratio of December - January to June-July abundances with latitude. Source references are given in Table II.

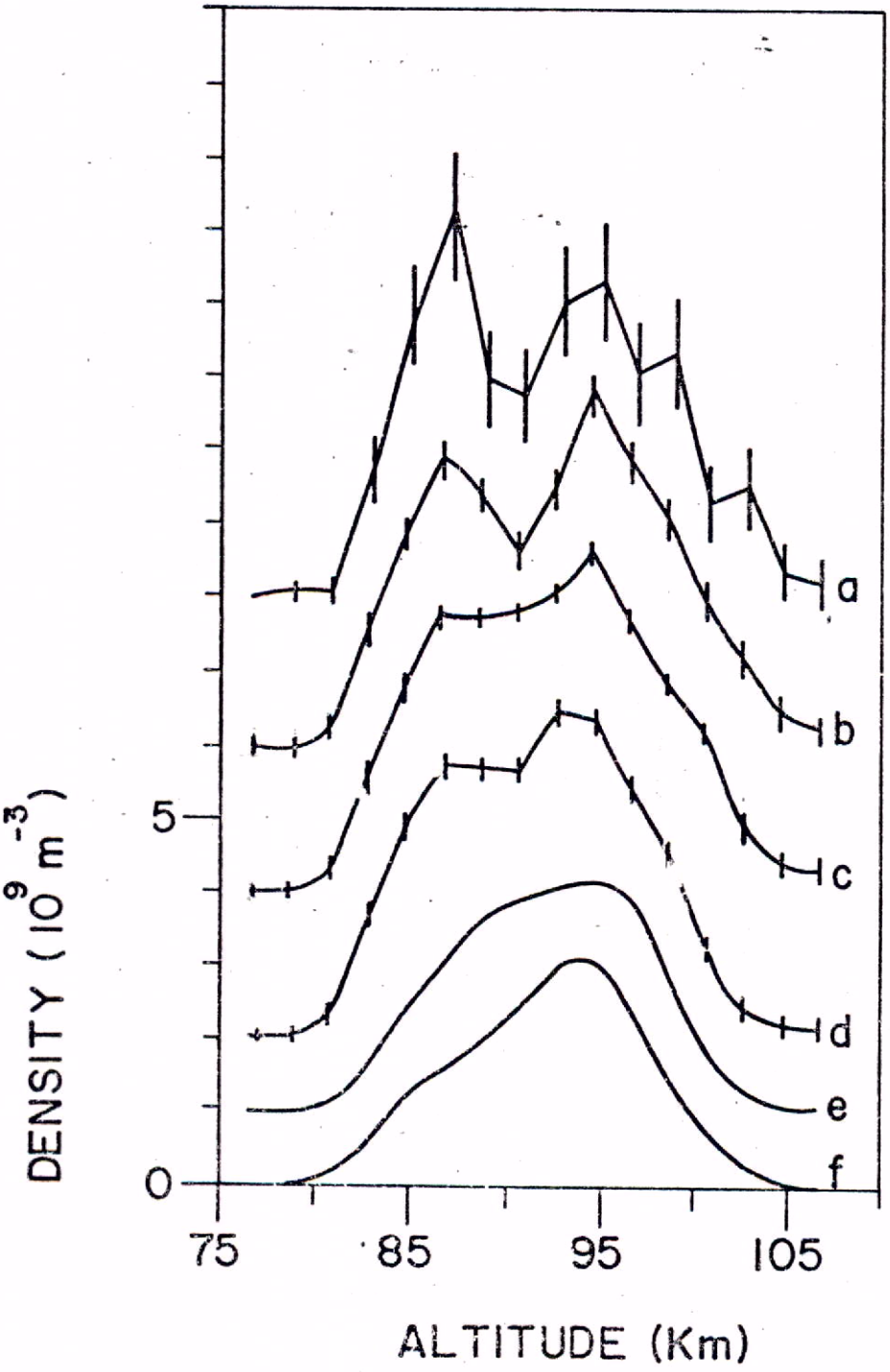

Fig. 1

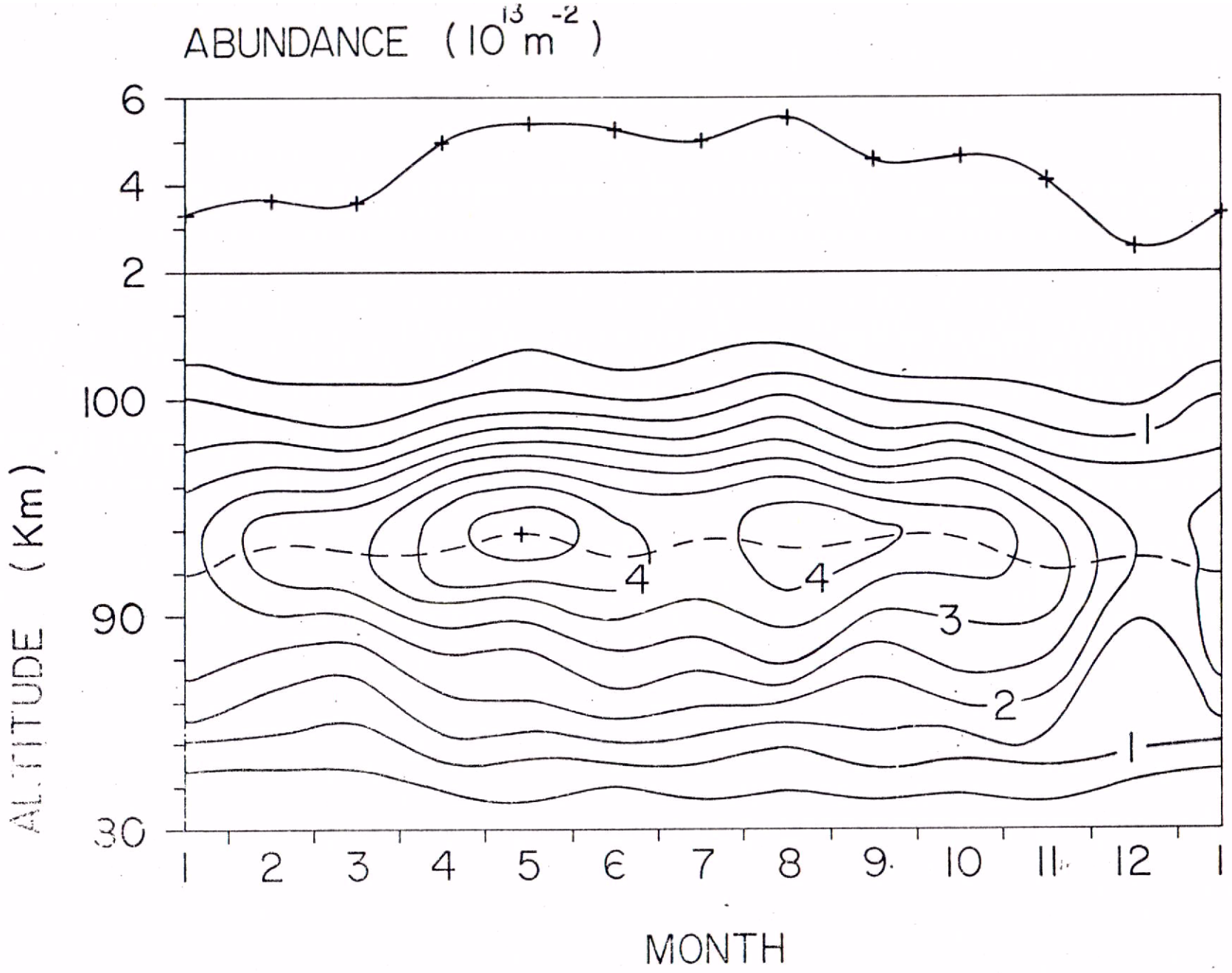
ABUNDANCE (10^{13} m^{-2})
6
4
2
100
90
30
ALTITUDE (Km)
1
4
4
3
2
1
1 2 3 4 5 6 7 8 9 10 11 12 1
MONTH

Fig. 2

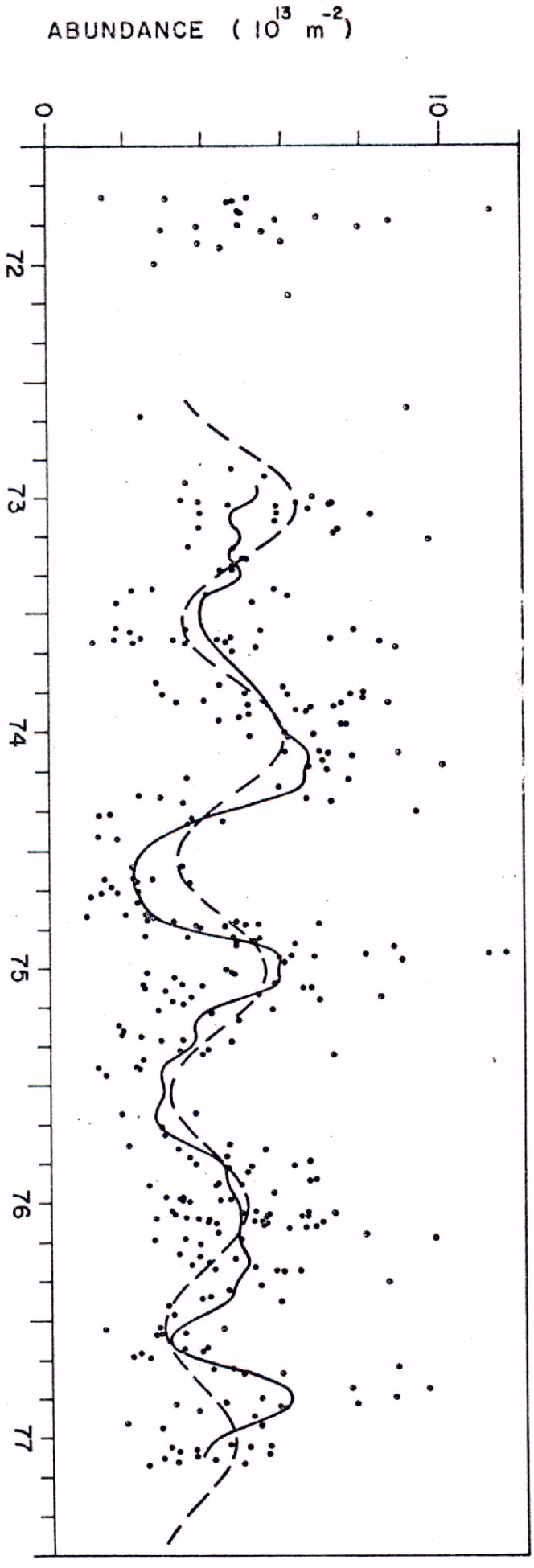

Fig. 3

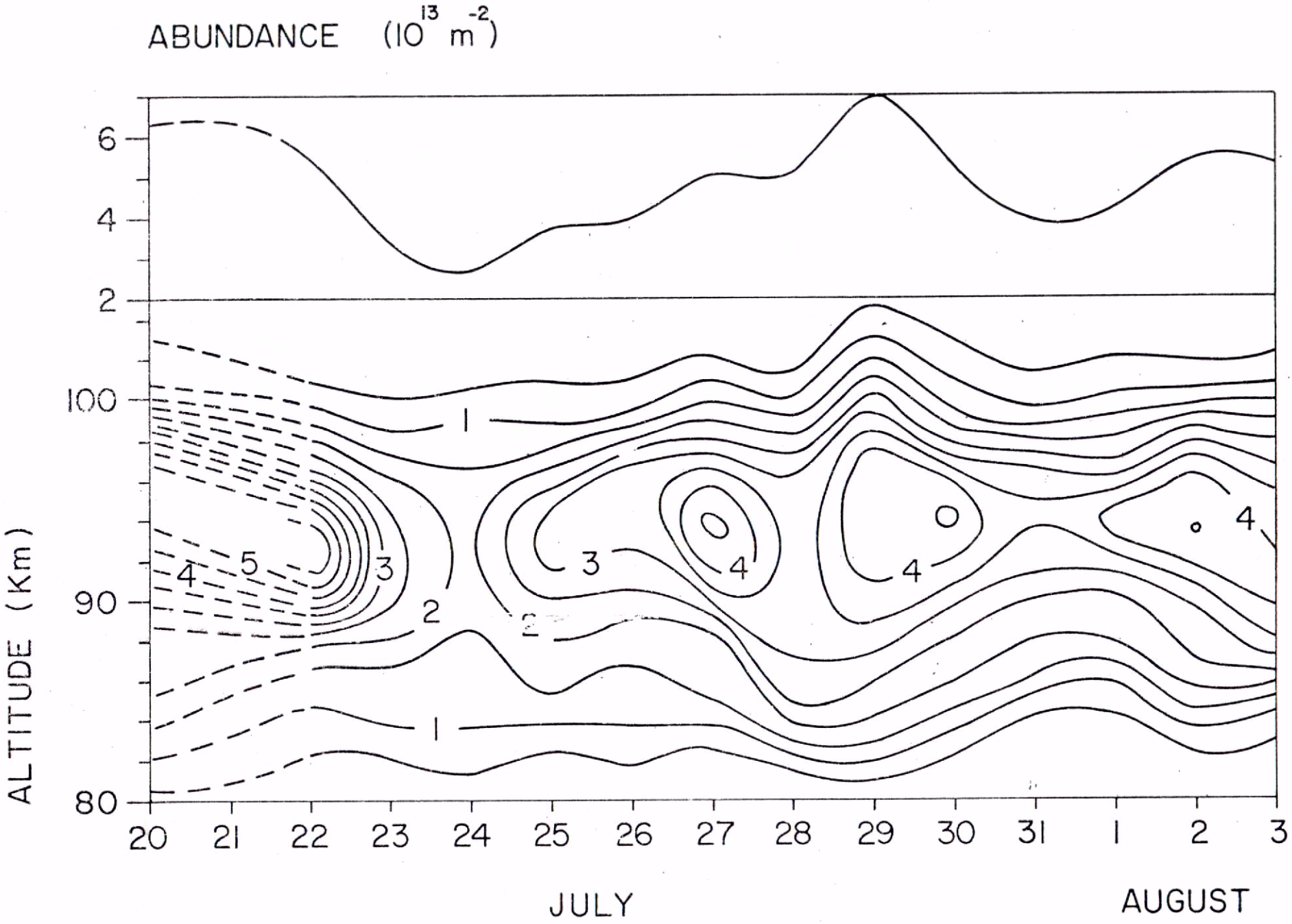
ABUNDANCE (10^13 m^-2)
6
4
2
100
90
80
ALTITUDE (Km)
1
5
4
3
2
3
4
4
0
4
1
20
21
22
23
24
25
26
27
28
29
30
31
1
2
3
JULY
AUGUST

Fig. 4

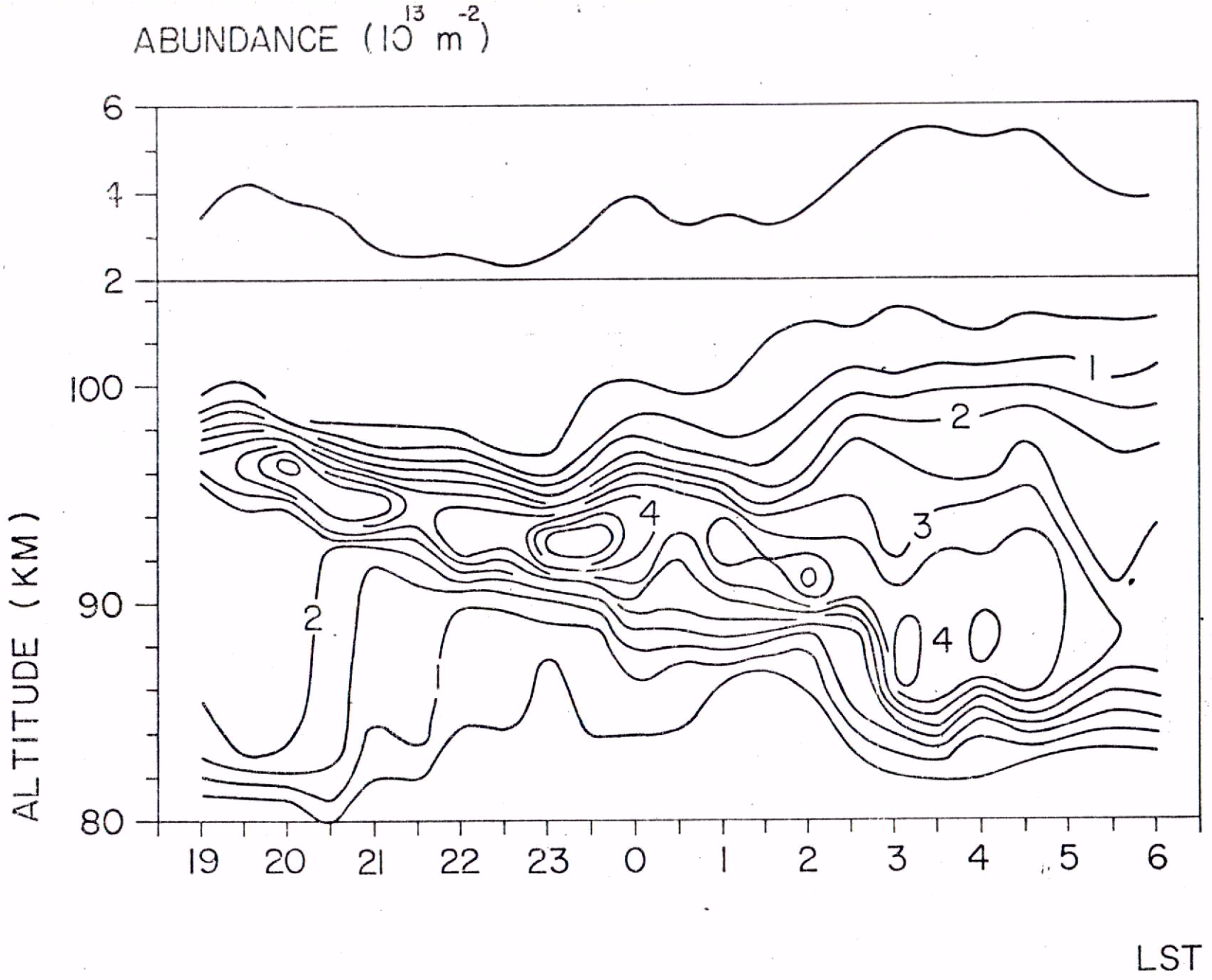
ABUNDANCE (10^{13} m^{-2})
6
4
2
100
90
80
ALTITUDE (KM)
1
2
3
4
0
19
20
21
22
23
0
1
2
3
4
5
6
LST

Fig. 5

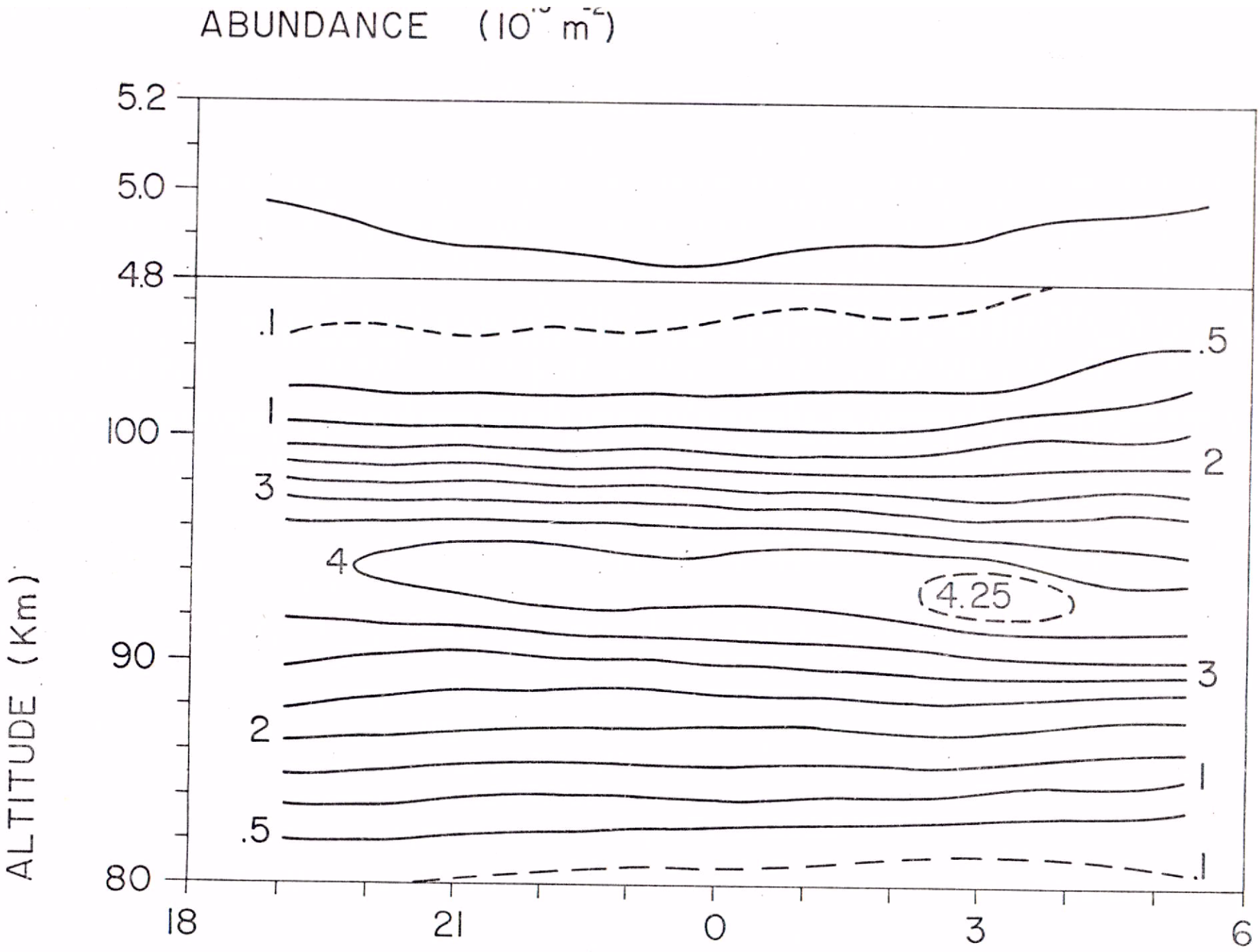
ABUNDANCE (10^9 m^-2)
5.2
5.0
4.8
100
90
80
ALTITUDE (Km)
.1
1
3
4
4.25
2
.5
.5
2
3
1
.1
18
21
0
3
6
LST

Fig. 6

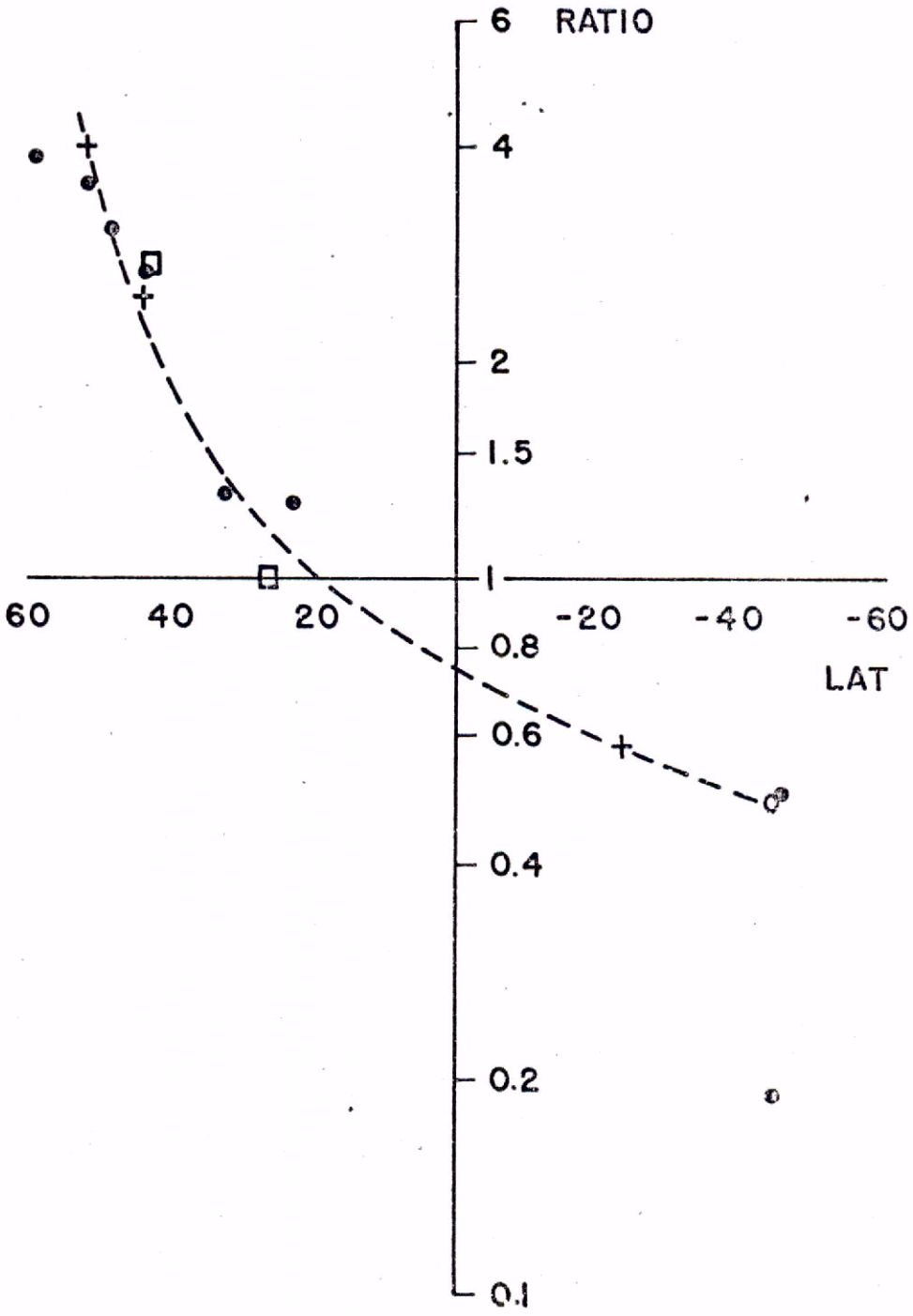

Fig. 7